

PRELIMINARY CRYSTALLOGRAPHIC ANALYSIS OF *LEISHMANIA SIAMENSIS* TRIOSEPHOSPHATE ISOMERASE COMPLEXED WITH ITS NOVEL INHIBITOR

Buabarn Kuaprasert,^{1,*} Jakrada Attarataya¹, Pinpunya Riangrunroj,² Wichai Pornthanakasem,² Wipa Suginta,³ Mathirut Mungthin,⁴ Soavane Leelayoova,⁴ Kiattawee Choowongkomon⁵, and Ubolsree Leartsakulpanich²

Received: September 21, 2015; Revised: November 04, 2015; Accepted: November 05, 2015

Abstract

Leishmania siamensis (*Ls*), a recently identified protozoan species that causes visceral leishmaniasis (VL), was isolated from a VL patient in Thailand. The putative gene encoding *L. siamensis* triosephosphate isomerase (*Ls*TIM) was cloned and heterologously expressed as an N-terminal hexa-histidine-tag fusion protein in *Escherichia coli*. The purified recombinant *Ls*TIM was found to fully function as a homodimeric enzyme, which could be crystallized and diffracted to the highest resolution of 1.93 Å using the rotating anode X-ray generator and 1.88 Å using the monochromatic X-ray from SLRI-beamline 7.2WLS at the Siam Photon Light Source. Chlorobiocin (NCI-227186), a novel inhibitor of *Ls*TIM, was co-crystallized successfully with the enzyme by the microbatch method. The complex crystal diffracted synchrotron light at SLRI-beamline 7.2WLS to the resolution of 2.50 Å. Our preliminary crystallographic data presented in this study would help in elucidating the specific inhibitory binding sites of *Ls*TIM that can be further designed as a drug target against VL.

Keywords: Triosephosphate isomerase, *Leishmania siamensis*, crystal structure, inhibitor

Introduction

Leishmaniasis is one of the zoonotic diseases caused by *Leishmania*, one of the trypanosomatid protozoan parasites. In humans, the disease occurs in at least four major forms: cutaneous, diffuse cutaneous, mucocutaneous, and visceral. Visceral leishmaniasis (VL), also known as kala-azar, becomes a public health threat in warm region countries, and is almost fatal if

¹ Research Facility Division, Synchrotron Light Research Institute (Public Organization), 111 University Avenue, Muang District, Nakhon Ratchasima, 30000, Thailand. E-mail: buabarn@slri.or.th

² National Center for Genetic Engineering and Biotechnology, 113 Paholyothin Rd., Klong Luang, Pathumthani, 12120, Thailand.

³ School of Biochemistry, Institute of Science, Suranaree University of Technology, 111 University Avenue, Muang District, Nakhon Ratchasima, 30000, Thailand.

⁴ Department of Parasitology, Phramongkutklao College of Medicine, Rachatewi, Bangkok, 10400, Thailand.

⁵ Department of Biochemistry, Faculty of Science, Kasetsart University, 50 Ngam Wong Wan Rd, Ladyaow, Chatuchak, Bangkok, 10900, Thailand.

* Corresponding author

left untreated. An estimated 12 million people are currently infected worldwide, and around 1.5-2.0 million new infections occur each year worldwide (World Health Organization, 2009). VL, the most severe form of leishmaniasis, is caused by *Leishmania* parasites of different species.

Leishmania and *Trypanosomes* are protozoa belonging to the Trypanosomatidea family, in which the first seven enzymes of the glycolytic pathway of the parasite are localized in glycosomes, which are not present in other eukaryote cells (Verlinde *et al.*, 2001). Bloodstream forms of the parasites exclusively rely on glucose metabolism; complete inhibition of any of glycolytic enzymes could combat the parasites (Oppendoes and Michels, 2008). Deletion of the TIM gene from *T. brucei* in an experiment and computer modeling of glycolytic pathway studies suggested that triosephosphate isomerase of bloodstream *Trypanosoma brucei* is the required TIM for parasite survival (Helfert *et al.* 2001). TIM (EC 5.3.1.1) is a glycolytic enzyme that catalyzes the isomerization of glyceraldehydes 3-phosphate (G3P) and dihydroxy-acetone phosphate (DHAP). It is usually formed by 2 identical monomers of approximately 250 amino acid residues. Each monomer comprises 8 central β strands, surrounded by 8 α helices which are connected together by loops to make up a TIM barrel structure. Temperature denaturation of *Trypanosoma cruzi* TIM in a study showed stable monomeric TIM with reduced activity (Schliebs *et al.*, 1996). Crystallographic structure observation of the conserved catalytic residues, Lys14, His96, and Glu168 revealed undistinguished differences in the active site of TIM from parasites and humans. However, designing a specific inhibitor against this enzyme became possible when the structure of the dimeric *T. cruzi* TIM crystal soaked in hexane was revealed. No major structural change was found, except that 2 molecules of hexane were located close to the residues that formed the dimer interface, such as Ile69, Arg71, Tyr75, Tyr103, Gly104, Ile109, and Lys113 from chain A, and Tyr102 and Tyr103 from chain B. This surface region, where no water

molecule was found in the native structure, was later called the “hydrophobic pocket” (Gao *et al.*, 1999). Disruption of the dimeric formation of the *T. cruzi* TIM enzyme by a small specific binding compound caused a dramatic loss of the catalytic activity (Tellez-Valencia *et al.*, 2004). Previous study revealed that 6,6'-bisbenzothiazole-2,2' diamine irreversibly inactivated the TIMs of *T. cruzi*, *T. brucei*, and *L. mexicana* at low micromolar concentrations, while this compound had no effect on TIMs from bacteria, yeast, plasmodium, chickens, and humans. The structural analysis results suggested that different effects of the inhibitor on different TIMs resulted from structural differences in the special pocket at the dimeric interface (Olivares-Illana *et al.*, 2006). Detailed inspection of the binding pocket at the dimeric interface of *T. cruzi* TIM led to intensive studies to find specific inhibitors. It has been reported that dithiodianiline (DTDA) induces conformation change of loop 3, located at the dimer interface, and results in completely inhibiting *Tc*TIM at the nanomolar concentration range (Olivares-Illana *et al.*, 2007). Moreover, 3 different chemotypes (1,2,6-thiadiazines, phenazine 5,9-dioxides, and thiazoles) from in-house synthesis library compounds have been identified as selective inhibitors for *Tc*TIM over *HT*TIM, and some of them enable the killing of the *T. cruzi* parasite in vitro (Alvarez *et al.*, 2010).

L. siamensis (MON - 324, WHO Code: MHOM/TH/2010/TR) (Bualert *et al.*, 2012; Leelayoova *et al.*, 2013) triosephosphate isomerase, *Ls*TIM, is a functional homodimeric enzyme and is highly conserved with TIM from other kinetoplastid protozoa. It shares a 91%, 87%, and 67% sequence identity with that from *L. infantum*, *L. mexicana*, and *T. cruzi*, respectively, and 49% with *human* TIM. Our study focused on the design of specific inhibitors against the unique binding pocket at the dimeric interface of *Ls*TIM. We recently succeeded in producing purified and crystallized *Ls*TIM. The crystal structure of the free-enzyme was solved to the highest resolution of 1.93 Å by the molecular replacement method using *T. cruzi* TIM (PDB Code: 1CI1 (Gao *et al.*,

1999)) as a search model (Kuaprasert *et al.*, 2015a). This structure was later used as a template for virtual screening against the National Cancer Institute compounds. The inhibitory screening of docked compounds at 100 μM indicated that chlorobiocin is one of the potential inhibitors (Kuaprasert *et al.*, 2015b). In this study, the X-ray diffraction data sets of the ligand-free enzyme and the enzyme complexes with chlorobiocin were obtained, and the preliminary crystallographic analyses are reported.

Materials and Methods

Protein expression and purification: In order to express the recombinant *LsTIM*, cells harboring the recombinant plasmid pET15b-*LsTIM* were grown at 310 K in LB medium containing 100 $\mu\text{g/ml}$ ampicillin, and protein expression was induced by the addition of isopropyl thio-D-galactoside (IPTG) when the cell culture reached an OD600 of approximately 0.8. Cell growth was continued at 289 K for 20 hours. About 4 g of cell paste was resuspended in buffer A (50 mM potassium phosphate buffer pH 8.0, 50 mM KCl, 50 mM imidazole, and 10% glycerol) and lysed with a French pressure cell at 69 MPa. The cell lysate was clarified twice by centrifugation at 27,000 g for 30 min. The crude extract was loaded onto a Ni-Sepaharose (GE Healthcare Life Sciences, Little Chalfont, UK) column previously equilibrated with buffer A. The column was extensively washed with buffer A until no protein was detected based on A280, followed by a stepwise elution of 30 ml each of buffer A containing 70, 100, 200, and 300 mM imidazole, respectively. The imidazole was removed with a Sephadex G25 gel filtration column previously equilibrated with a 50 mM potassium phosphate buffer pH 8.0, 50 mM KCl, 5 mM DTT, and 10% glycerol. The protein was concentrated by ultrafiltration (Amicon, Sigma-Aldrich Corp., St. Louis, MO, USA) with a 10 kDa cutoff membrane. No attempt was made to remove the hexa-histidine tag prior to crystallization. The salts and glycerol were from Scharlau Chemicals (Scharlab, S.L.,

Barcelona, Spain).

Crystallization and X-ray diffraction using home source X-ray: Crystallization trials for the hexa-histidine tagged *LsTIM* were done by the microbatch method in Douglas Vapor Batch 96-well plates (Douglas Instruments, Ltd., Hungerford, UK) at 291 K. Crystallization drops contained equal volumes (1.0 μl) of precipitant and enzyme (25.4 mg/ml) solutions under 5.0 μl of oil (BabiMild Sweety Pink Plus, Osotspa Co., Ltd., Bangkok, Thailand). Single crystals were obtained from crystal screening using Crystal Screen (HR2-110) from Hampton Research Corp., Aliso Viejo, CA, USA: 0.2M calcium acetate hydrate and 0.1M sodium cacodylate trihydrate, pH 6.5, and 18% PEG8000 used as the precipitating reagent. Each crystal was prepared for cryocrystallography by harvesting the crystal directly into a nitrogen gas cryostream. X-ray diffraction data was collected under 100 K in the nitrogen flow from a Cryostream Cooler (Oxford Cryosystems Ltd., Long Hanborough, UK), with a Cu $K\alpha$ rotating-anode source mounted on a MicroSTAR X-ray generator (Bruker AXS GmbH, Karlsruhe, Germany) operating at 45 kV and 60 mA. A total of 159 1.0 oscillation images were exposed for 6 min each (Table 1).

Crystal optimization and X-ray diffraction using synchrotron X-ray: To improve the X-ray diffraction quality, crystal optimization by the microbatch method, with the same details as mentioned previously, was performed with varying pHs and PEG8000 concentrations nearby an initial precipitating condition; 5.9-6.5 and 18–22% w/v for the pHs and PEG8000 concentrations, respectively. The crystallization drops contained equal volumes (1.0 μl) of precipitant and enzyme (24.2 mg/ml in 50 mM potassium phosphate buffer, pH 8.0, containing 50 mM KCl, 5 mM DTT, and 10% glycerol). The best single crystal grown under 0.2 mM calcium acetate hydrate, 0.1 M sodium cacodylate trihydrate, pH 5.9, and PEG8000 18% w/v within 2 days was mounted on a goniometer under 100 K cryostream with a 90 mm crystal-to-detector distance prior to the X-ray diffraction experiment. Utilizing the X-ray from SLRI-beamline 7.2WLS ($\lambda = 1.550\text{\AA}$),

(a Rayonix SX-165 CCD detector mounted on a MarDTB, operating under the Synchrotron Light Research Institute (Public Organization) (SLRI), Nakhon Ratchasima, Thailand), a total of 130 images were collected successfully with 40 seconds exposure time per one 1.0 oscillation image. Under these conditions, the crystal diffracted the X-rays to beyond 1.88 Å (Table 1). The data were processed by using iMOSFLM (Battye *et al.*, 2011). The chemicals for the crystallization optimization were from Sigma-Aldrich Corp.

LsTIM-NCI-227186 complex: Co-crystallization of the LsTIM and NCI-227186 compound was carried out under the optimization conditions mentioned above, but equal volumes (1.0 µl) of precipitant, protein, and NCI-227186 (50mM dissolved in 100% dimethyl sulfoxide (DMSO)) were applied for setting a crystallizing drop. The crystal grew within 2 days and diffracted the X-ray at SLRI-beamline 7.2WLS. More details are shown in Table 1.

LsTIM hydrophobic pocket identification: A unique LsTIM hydrophobic pocket was identified by PyMOL structural alignment software (DeLano, 2005) of LsTIM (Kuaprasert *et al.*, 2015a) with related enzymes from *T. cruzi* in hexane (PDB Code: 1CI1) and human blood (PDB Code: 2JK2 (Rodriguez-Almazan *et al.*, 2008)) for further receptor-based virtual screening.

Receptor-based virtual screening of LsTIM against National Cancer Institute (NCI) Diversity Database: The virtual screening was calculated by using the AutoDock program V.4.0. The NCI diversity was obtained from <http://zinc.docking.org/browse/catalogs/all> containing 1,364 compounds. An unpublished crystal structure of LsTIM was set as the target protein to screen the ligands from the NCI diversity. The docking process consisted of sampling the co-ordinate space around the binding site and scoring each possible ligand pose, which was then taken as the predicted

binding mode for each compound. For the parameter setting, the rotational bonds of all proteins were regarded as being rigid, while the rotational bonds of the ligands were treated as flexible. The hydrogen atoms, the Kollman united-atom charges, and the solvent parameter were applied to the proteins, and the set-up process for the grid was performed in Auto DockTools V.1.5.2. A grid box was built with 12 different atom types via AutoGrid calculations. The grid space was set at 0.375 Å. The AutoDock calculation was performed 50 times per ligand. The 40 best-hit compounds were selected by the lowest binding energy (AutoDock4 score). The interactions between the LsTIM and ligands were observed by using the Swiss-PdbViewer V4.0.1. The molecular modeling figures were made by PyMOL.

LsTIM activity determination and an initial inhibitory test: To measure the LsTIM activity, the LsTIM was assayed spectrophotometrically for the formation of DHAP by coupling the LsTIM reaction with the α -glycerophosphate dehydrogenase (GPDH) reaction. The LsTIM converts GAP to DHAP, which will be reduced to glycerol-3-phosphate by GPDH in the presence of NADH. The consumption of NADH was monitored at absorbance 340 nm ($\epsilon_{340} = 6.22 /\text{mM}\cdot\text{cm}$). The assay solution (1 mL) contained 100 mM triethanolamine-HCl, pH 7.5, 10 mM EDTA, 200 mM GAP, 0.3 mM NADH, 24 µg (3.12 units) of GPDH, and LsTIM. One unit of LsTIM activity is defined as the amount of the enzyme that catalyzes GAP 1 µmol per minute at 25°C.

Forty hits of the NCI compounds were purchased from the NCI. All of them were dissolved in 100% DMSO. A 100 µM concentration of these compounds was used for an initial LsTIM inhibitory screening in an excess of α -glycerophosphate dehydrogenase (GPDH), a coupling enzyme. The reaction with DMSO with an equal volume was used as a control. The chemicals for the activity assay were from Sigma-Aldrich Corp.

Table 1. Crystallization conditions, data collection parameters and X-ray data statistics

Numbers in parenthesis are in the highest resolution shell.

	Free LsTIM form 1	Free LsTIM form 2	LsTIM- NCI227186
<i>Crystallization parameters</i>			
Protein buffer	50 mM K ₂ PO ₄ buffer, pH 8.0, 50 mM NaCl, 5 mM DTT and 10% glycerol	50 mM K ₂ PO ₄ buffer, pH 8.0, 50 mM KCl, 5 mM DTT and 10% glycerol	50 mM K ₂ PO ₄ buffer, pH 8.0, 50 mM KCl, 5 mM DTT and 10% glycerol
<i>Crystallization condition</i>	0.2 mM Calcium acetate hydrate and 0.1 M Sodium cacodylate trihydrate	0.2 mM Calcium Acetate hydrate and 0.1 M Sodium cacodylate trihydrate	0.2 mM Calcium acetate hydrate and 0.1 M Sodium cacodylate trihydratexs
pH	6.5	5.9	6.3
PEG8000	18%	18%	22%
Co-inhibitor method	free-protein	free-protein	Co-crystallization
Temperature	291K	291K	291K
<i>Data collection parameters</i>			
Crystal to detector distance (mm)	70	70	90
Exposure time (s)	360	40	40
Oscillation range (°)	1.0	1.0	1.0
No. of frames	159	130	180
Wavelength (Å)	1.482	1.550	1.550
X-ray source	Rotating anode X-ray generator	SLRI-beamline 7.2WLS	SLRI-beamline 7.2WLS
<i>X-ray data statistics</i>			
Resolution (Å)	21.61-1.93 (1.98-1.88)	(2.03-1.93) 27.60-2.50	21.56-1.88 (2.64-2.5)
Space group	<i>P</i> 1 2 1	<i>C</i> 2	<i>P</i> 1 21 1
Mosaicity	0.48	0.53	0.59
Unit-cell parameters (Å)	39.58, 78.79, 83.16 90.00, 101.15, 90.00	81.44, 76.45, 94.94 90.00, 101.14, 90.00	39.60, 78.39, 82.94 90.00, 100.94, 90.00
Unit-cell angles (°)			
Observed reflections	117,395 (15,450)	130,315 (6,430)	63,912
Unique reflections	33,449(4,911)	46,160 (2,463)	17,063
Multiplicity	3.3 (3.1)	2.8 (2.6)	3.7 (3.7)
Mean I/sigma (I)	14.2 (3.1)	11.9 (2.4)	10.1 (5.3)
Completeness (%)	93.2 (90.2)	98.6 (81.2)	97.4 (98.6)
Rmerge (%)	5.4 (20.2)	0.07 (0.50)	10.2 (23.2)
Matthew Coefficient	2.18	2.48	2.16
No. of molecule/ASU	2	2	2
Solvent content (%)	43.55	50.49	43.01

Results and Discussion

Initial crystals of *LsTIM* were achieved from a preliminary screen using Crystal Screen (HR2-110) from Hampton Research Ltd.: 0.2 M calcium acetate hydrate and 0.1 M sodium cacodylate trihydrate, pH 6.5, and 18% PEG8000 used as the precipitating reagent. A crystal was then taken for X-ray diffraction under liquid nitrogen cryostream using the home source. The crystallizing solution acted as a suitable cryoprotectant and the crystal diffracted the X-ray to the highest resolution of 1.93 Å and belonged to the monoclinic *P121* space group (Kuaprasert *et al.*, 2015a). To improve the crystal quality, optimization with varying precipitating solutions, pH, and PEG8000 concentration steps was performed using the microbatch method. Single crystals of free-*LsTIM* were successfully grown under the condition containing 0.2 mM calcium acetate hydrate, 0.1 M sodium cacodylate trihydrate, pH 5.9, and 18% PEG8000. The best crystal was shown to diffract synchrotron light to the highest resolution of 1.88 Å. The protein crystals and diffraction pattern are presented in Figure 1. Ligand-free *LsTIM* crystals belong to monoclinic space groups. Replacing sodium salt with potassium salt in a protein buffer may

cause the space group *P121* to change to a higher symmetry face-centered *C2* space group (Figure 2). X-ray diffraction using synchrotron light at SLRI-beamline 7.2WLS ($\lambda = 1.550$ Å) slightly improved the resolution of the crystal structure over the in-house X-ray source ($\lambda = 1.482$ Å). This may be caused by a shorter exposure time, which reduced the radiation damage in the crystal. It seems that the ligand-free protein crystals diffracted the X-ray beam to better resolutions than that of the complex crystal. It is likely that the presence of an inhibitor in the crystallization solution changed the molecular packing from the *C2* to *P1211* space group (Table 1).

Structural comparisons of *LsTIM*, *TcTIM*, and *HTIM* indicate that conserved residues related to hexane binding in the *TcTIM* structure are remarkably similar to that of *LsTIM* (Ile69, Phe75, Tyr102, Tyr103, Gly104, and Lys113). Only 2 amino acid residues are different, Lys71 and Val109 for *LsTIM* and Arg71 and Ile109 for *TcTIM*. In contrast, there are Tyr69, Val71, Phe75, Val102, Phe103, Gly104, Lue109, and Lys113 existent in *HTIM*, and they caused significant size and space pocket differences to that of TIM from *T. cruzi* and *L. siamensis* (Figure 3). This pocket was then used for a receptor-based virtual

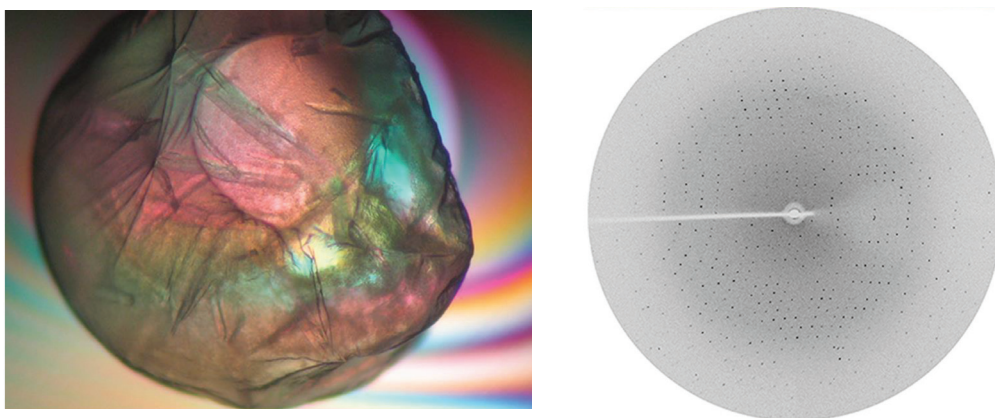


Figure 1. Crystals of *LsTIM* in microbatch drop with crystallizing condition containing 0.2 mM calcium acetate hydrate, 0.1 M sodium cacodylate trihydrate, pH 5.9, and 18% PEG8000 (Left); X-ray diffraction pattern of *LsTIM* crystal at 1.88 Å (Right)

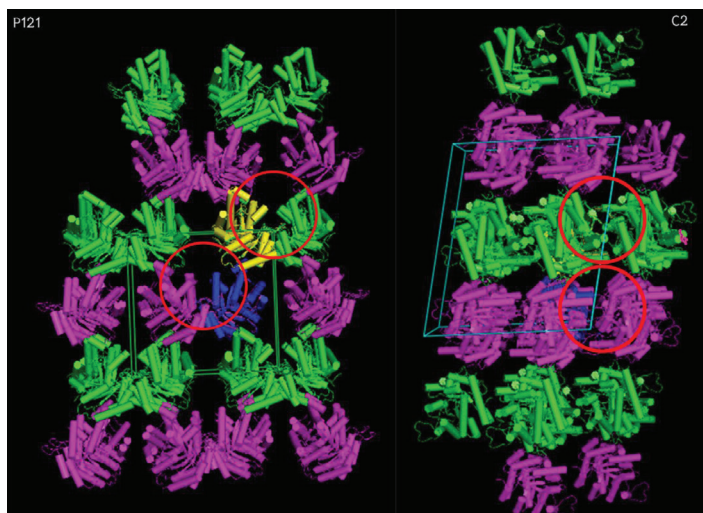


Figure 2. Dimeric interface region is clearly seen in *LsTIM* crystal packing in *P121* space group (Left) and *C2* (Right). Cartoon representations in yellow and blue are *LsTIM* chain A and B that make dimeric interaction with an identical adjacent molecule, represented in green and magenta, respectively. Red circles indicate the region, created by the 2 adjacent molecules connected together, where an inhibitor is assumed to bind

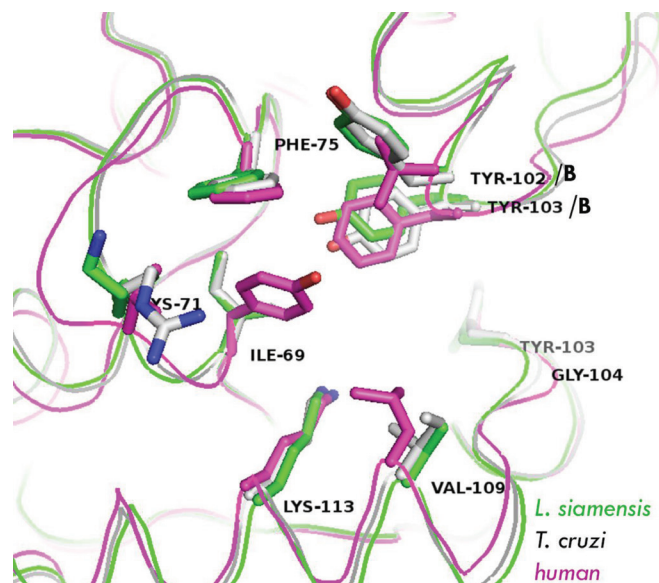


Figure 3. Structural comparisons of hydrophobic pockets of TIMs from *L. siamensis* (green) and *T. cruzi* (magenta); they are significantly different from that of *HTIM* (grey) in which Tyr69 is pointing into the middle pocket space. The designed compound with best fit parasitic pocket enzyme may not affect the related human enzyme. The labeled residue numbers belong to *LsTIM*. The pocket is made of amino acids from 2 subunits where Ile69, Lys71, Phe75, Tyr103, Gly104, Val109, and Lys113 are from subunit A while Tyr 102 and Tyr 103 are from subunit B

screening, and the result suggested potential NCI compounds that could bind the enzyme. Chlorobiocin was found to inhibit *LsTIM* activity by 43% in an initial 100 μ M inhibitor screening. Although chlorobiocin is assumed to bind *LsTIM* at the hydrophobic binding site, insight into the inhibitor bound enzyme is needed for further seeking chlorobiocin sub-structure modification possibilities to improve tight binding compounds.

In order to get the enzyme-inhibitor complex, co-crystallization of 60:1 mole ratio of inhibitor to enzyme was applied for setting a crystallizing drop in the microbatch optimization method. The best complex crystal obtained from the condition containing 0.2 mM calcium acetate hydrate, 0.1 M sodium cacodylate trihydrate, pH 6.3, and 22% PEG8000, diffracted the synchrotron radiation to the highest resolution of 2.50 Å. Details of the crystallization, data collection parameters, and X-ray data statistics are shown in Table 1. Phase analysis of the chlorobiocin bound enzyme structure is underway.

Conclusions

Triosephosphate isomerase is one of the glycolytic enzymes that have been structurally and functionally studied intensively in kinetoplastid protozoa, such as *T. cruzi*. (which causes Chagas disease), *T. brucei* (which causes sleeping sickness) and *L. mexicana* (which causes Leishmaniasis). Leishmaniasis, in particular, is a subject of major concern for public health problems in tropical and sub-tropical countries, since there is no vaccine or low cost effective drugs available against the disease. Although Leishmaniasis is not a common disease and is rarely found in Thailand, the discovery of *L. siamensis*, which causes VL, indicates that the disease is widespread and re-emerging in Thailand. Structural analysis showed that the inhibitory binding site of *LsTIM* was different from that of *HTIM*. These data will provide useful information for the structural-based design of tight binding inhibitors for a possible cure of VL in the future.

Acknowledgements

This project is financially supported by the Synchrotron Light Research Institute (Public Organization) (SLRI: GRANT 2 - 2549/LS01) and National Center for Genetic Engineering and Biotechnology (BIOTEC), Thailand (P - 00 - 0029). Dr. Penchit Chitnumsub is grateful for valuable discussions. All staff members at SLRI-beamline7.2WLS are appreciated for their assistance during data collection.

References

- Alvarez, G., Aguirre-Lopez, B., Varela, J., Cabrera, M., Merlino, A., Lopez, G.V., Lavaggi, M.L., Porcal, W., Di Maio, R., Gonzalez, M., Cerecetto, H., Cabrera, N., Perez-Montfort, R., de Gomez-Puyou, M.T., and Gomez-Puyou, A. (2010). Massive screening yields novel and selective *Trypanosoma cruzi* triosephosphate isomerase dimer-interface-irreversible inhibitors with anti-trypanosomal activity. *Eur. J. Med. Chem.*, 45:5767-5772.
- Battye, T.G., Kontogiannis, L., Johnson, O., Powell, H.R., and Leslie, A.G.W. (2011). iMOSFLM: a new graphical interface for diffraction-image processing with MOSFLM. *Acta Crystallogr. D*, 67:271-281.
- Bualert, L., Charungkiattikul, W., Thongsuksai, P., Mungthin, M., Siripattanapipong, S., Khositnithikul, R., Naaglor, T., Ravel, C., El Baidouri, F., and Leelayoova, S. (2012). Autochthonous disseminated dermal and visceral Leishmaniasis in an AIDS patient, Southern Thailand, caused by *Leishmania siamensis*. *Am. J. Trop. Med. Hyg.*, 86:821-824.
- DeLano, W. L. (2005). PyMOL.
- Gao, X.G., Maldonado, E., Perez-Montfort, R., Garza-Ramos, G., De Gomez-Puyou, M.T., Gomez-Puyou, A., and Rodriguez-Romero, A. (1999). Crystal structure of triosephosphate isomerase from *Trypanosoma cruzi* in hexane. *P.Natl Acad. Sci. USA*, 96:10062-10067.
- Helfert, S., Estevez, A.M., Bakker, B., Michels, P.A.M., and Clayton, C. (2001). Roles of triosephosphate isomerase and aerobic metabolism in *Trypanosoma brucei*. *Biochem. J.*, 357:117-125.
- Kuaprasert, B., Riangrunroj, P., Pornthanakasem, W., Attarataya, J., Sirimontree, P., Suginta, W., Mungthin, M., Leelayoova, S., Choowongkamon, K., and Leartsakulpanich, U. (2015a). Unpublished data. Synchrotron Light Research Institute (Public

- Organization). 111 University Avenue, Muang District, Nakhon Ratchasima, 30000, Thailand.
- Kuaprasert, B., Riengrunroj, P., Pornthanakasem, W., Mungthin, M., Leelayoova, S., Choowongkamon, K., and Leartsakulpanich, U. (2015b). Crystal structure of *Leishmania siamensis* triosephosphate isomerase and its receptor-based virtual screening NCI inhibitors [abstract]. SLRI Annual User Meeting 2015; 19 January 2015; Bangkok, Thailand, p. 10-11. Abstract no. 30.
- Leelayoova, S., Siripattanapipong, S., Hitakarun, A., Kato, H., Tan-ariya, P., Siriyasatien, P., Osatakul, S., and Mungthin, M. (2013). Multilocus characterization and phylogenetic analysis of *Leishmania siamensis* isolated from autochthonous visceral leishmaniasis cases, southern Thailand. *BMC Microbiology*, 13:60.
- Olivares-Illana, V., Perez-Montfort, R., Lopez-Calahorra, F., Costas, M., Rodriguez-Romero, A., Tuena de Gomez-Puyou, M., and Gomez-Puyou, A. (2006). Structural differences in triosephosphate isomerase from different species and discovery of a multitypanosomatid inhibitor. *Biochemistry*, 45:2556-2560.
- Olivares-Illana, V., Rodriguez-Romero, A., Becker, I., Berzunza, M., Garcia, J., Perez-Montfort, R., Cabrera, N., Lopez-Calahorra, F., Tuena de Gomez-Puyou, M., and Gomez-Puyou, A. (2007). Perturbation of the dimer interface of triosephosphate isomerase and its effect on *Trypanosoma cruzi*. *PLOS Neglect. Trop. D.*, 1(1):e1.
- Opperdoes, F. R. and Michels, P.A.M. (2008). The metabolic repertoire of *Leishmania* and implications for drug discovery. In *Leishmania: After the Genome*. Myler, P.J. and Fasel, N., (eds). Caister Academic Press, Wymondham, UK, p. 123-144.
- Rodriguez-Almazan, C., Arreola, R., Rodriguez-Larrea, D., Aguirre-Lopez, B., Tuena de Gomez-Puyou, M., Perez-Montfort, R., Costas, M., Gomez-Puyou, A., and Torres-Larios, A. (2008). Structural basis of human triosephosphate isomerase deficiency: mutation of E104D is related to alterations of conserved water network at the dimer interface. *J. Biol. Chem.*, 283:23254-23263.
- Schliebs, W., Thanki, N., Eritja, R., and Wierenga, R. (1996). Active site properties of monomeric triosephosphate isomerase (monoTIM) as deduced from mutational and structural studies. *Protein Sci.*, 5:229-239.
- Tellez-Valencia, A., Olivares-Illana, V., Hernandez-Santoyo, A., Perez-Montfort, R., Costas, M., Rodriguez-Romero, A., Lopez-Calahorra, F., De Gomez-Puyou, M.T., and Gomez-Puyou, A. (2004). Inactivation of triosephosphate isomerase from *Trypanosoma cruzi* by an agent that perturbs its dimer interface. *J. Mol. Biol.*, 341:1355-1365.
- Verlinde, C.L.M.J., Hannaert, V., Blonski, C., Willson, M., Perie, J.J., Fothergill-Gilmore, L.A., Opperdoes, F.R., Gelb, M.H., Hol, W.G.J., and Michels, P.A.M. (2001). Glycolysis as a target for the design of new anti-trypanosome drugs. *Drug Resist. Update.*, 4:50-65.
- World Health Organization. (2009). *Global Plan to Combat Neglected Tropical Diseases 2008-2015*. Geneva, Switzerland.

